



QUIDEL

## MicroVue Pan-Specific C3 Reagent Kit

Expand the arsenal of Complement analysis in animals with the ability to detect depletion of C3.

Find out how this kit fills the gap of animal-specific Complement ELISA.



## Enhancement of Tumor-Specific T Cell–Mediated Immunity in Dendritic Cell–Based Vaccines by *Mycobacterium tuberculosis* Heat Shock Protein X

This information is current as of December 8, 2014.

In Duk Jung, Sung Jae Shin, Min-Goo Lee, Tae Heung Kang, Hee Dong Han, Seung Jun Lee, Woo Sik Kim, Hong Min Kim, Won Sun Park, Han Wool Kim, Cheol-Heui Yun, Eun Kyung Lee, T.-C. Wu and Yeong-Min Park

*J Immunol* 2014; 193:1233-1245; Prepublished online 2 July 2014;

doi: 10.4049/jimmunol.1400656

<http://www.jimmunol.org/content/193/3/1233>

**Supplementary Material** <http://www.jimmunol.org/content/suppl/2014/07/02/jimmunol.1400656.DCSupplemental.html>

**References** This article **cites 25 articles**, 11 of which you can access for free at: <http://www.jimmunol.org/content/193/3/1233.full#ref-list-1>

**Subscriptions** Information about subscribing to *The Journal of Immunology* is online at: <http://jimmunol.org/subscriptions>

**Permissions** Submit copyright permission requests at: <http://www.aai.org/ji/copyright.html>

**Author Choice** Freely available online through *The Journal of Immunology* [Author Choice option](#)

**Email Alerts** Receive free email-alerts when new articles cite this article. Sign up at: <http://jimmunol.org/cgi/alerts/etoc>

*The Journal of Immunology* is published twice each month by The American Association of Immunologists, Inc., 9650 Rockville Pike, Bethesda, MD 20814-3994. Copyright © 2014 by The American Association of Immunologists, Inc. All rights reserved. Print ISSN: 0022-1767 Online ISSN: 1550-6606.



# Enhancement of Tumor-Specific T Cell–Mediated Immunity in Dendritic Cell–Based Vaccines by *Mycobacterium tuberculosis* Heat Shock Protein X

In Duk Jung,<sup>\*,1</sup> Sung Jae Shin,<sup>†,1</sup> Min-Goo Lee,<sup>‡</sup> Tae Heung Kang,<sup>\*</sup> Hee Dong Han,<sup>\*</sup> Seung Jun Lee,<sup>\*</sup> Woo Sik Kim,<sup>†</sup> Hong Min Kim,<sup>†</sup> Won Sun Park,<sup>§</sup> Han Wool Kim,<sup>¶,||</sup> Cheol-Heui Yun,<sup>¶,||</sup> Eun Kyung Lee,<sup>#</sup> T.-C. Wu,<sup>\*\*,††,‡‡,§§</sup> and Yeong-Min Park<sup>\*</sup>

Despite the potential for stimulation of robust antitumor immunity by dendritic cells (DCs), clinical applications of DC-based immunotherapy are limited by the low potency in generating tumor Ag-specific T cell responses. Therefore, optimal conditions for generating potent immunostimulatory DCs that overcome tolerance and suppression are key factors in DC-based tumor immunotherapy. In this study, we demonstrate that use of the *Mycobacterium tuberculosis* heat shock protein X (HspX) as an immunoadjuvant in DC-based tumor immunotherapy has significant potential in therapeutics. In particular, the treatment aids the induction of tumor-reactive T cell responses, especially tumor-specific CTLs. The HspX protein induces DC maturation and proinflammatory cytokine production (TNF- $\alpha$ , IL-1 $\beta$ , IL-6, and IFN- $\beta$ ) through TLR4 binding partially mediated by both the MyD88 and the TRIF signaling pathways. We employed two models of tumor progression and metastasis to evaluate HspX-stimulated DCs in vivo. The administration of HspX-stimulated DCs increased the activation of naive T cells, effectively polarizing the CD4<sup>+</sup> and CD8<sup>+</sup> T cells to secrete IFN- $\gamma$ , as well as enhanced the cytotoxicity of splenocytes against HPV-16 E7 (E7)–expressing TC-1 murine tumor cells in therapeutic experimental animals. Moreover, the metastatic capacity of B16-BL6 melanoma cancer cells toward the lungs was remarkably attenuated in mice that received HspX-stimulated DCs. In conclusion, the high therapeutic response rates with tumor-targeted Th1-type T cell immunity as a result of HspX-stimulated DCs in two models suggest that HspX harnesses the exquisite immunological power and specificity of DCs for the treatment of tumors. *The Journal of Immunology*, 2014, 193: 1233–1245.

**E**pidemiological studies analyzing the causes of cancer often provide clues regarding effective prevention and treatment methods. Indeed, the epidemiological research investigating the bacillus Calmette–Guérin (BCG) vaccination against tuberculosis (TB) and the occurrence of cancer has shown a lower rate of occurrence of certain cancers in people who had developed an effective level of immunity as a result of receiving the BCG vaccine (1). Over the past 20 y, there has been continuous research into cancer immunotherapy aimed at enhancing the effects of innate immunity and CTLs using the BCG vaccine. In particular, research is actively analyzing pathogen-associated molecular patterns, the role of the pattern recognition receptors known as TLRs, the cross-reactivity of Ags observed in cancer and germs and viruses, and the development of adjuvants that boost innate immune responses.

It is well known that dendritic cells (DCs) regulate the activity of CTLs in innate and adaptive immune responses, which play crucial roles in cancer immunotherapy (2). In addition, DCs are the APCs in immunotherapy that can effectively present the Ag of a vaccine. Recently, it has been reported that certain Ags of the BCG vaccine can activate DCs through the TLR4 and TLR2 pathways and increase the differentiation and activity of CTLs (3–7). Previously, we reported an increase in the survival rate in an E.G7 thymoma model in which mice were vaccinated with DCs, and heparin-binding hemagglutinin protein extracted from *Mycobacterium tuberculosis* was used to stimulate the TLR4 levels (6). *M. tuberculosis* consists of various proteins that are involved in the maturation and activation of DCs, and during a screen for DC activators within the mycobacterial Ag, we identified heat shock protein X (HspX) as the strongest TLR4 agonist.

<sup>\*</sup>Department of Immunology, Laboratory of Dendritic Cell Differentiation and Regulation, School of Medicine, Konkuk University, Chungju 380-701, South Korea; <sup>†</sup>Department of Microbiology, Institute for Immunology and Immunological Diseases, Brain Korea 21 PLUS Project for Medical Science, Yonsei University College of Medicine, Seoul 120-752, South Korea; <sup>‡</sup>Department of Physiology, College of Medicine, Korea University, Seoul 136-705, South Korea; <sup>§</sup>Department of Physiology, School of Medicine, Kangwon National University, Chuncheon 200-701, South Korea; <sup>¶</sup>Department of Agricultural Biotechnology, Seoul National University, Seoul 151-921, South Korea; <sup>||</sup>Research Institute for Agriculture and Life Sciences, Seoul National University, Seoul 151-921, South Korea; <sup>#</sup>Yongsan Hospital College of Medicine, Chung-Ang University, Seoul 156-756, South Korea; <sup>\*\*</sup>Department of Pathology, Johns Hopkins Medical Institutions, Baltimore, MD 21205; <sup>††</sup>Department of Obstetrics and Gynecology, Johns Hopkins Medical Institutions, Baltimore, MD 21205; <sup>‡‡</sup>Department of Molecular Microbiology and Immunology, Johns Hopkins Medical Institutions, Baltimore, MD 21205; and <sup>§§</sup>Department of Oncology, Johns Hopkins Medical Institutions, Baltimore, MD 21205

<sup>1</sup>I.D.J. and S.J.S. contributed equally to this work.

Received for publication March 18, 2014. Accepted for publication May 28, 2014.

This work was supported by National Research Foundation of Korea Grant NRF-2012R1A2A1A03008433 funded by the Korean Government and Cervical Cancer Specialized Program of Research Excellence Grant P50CA098252.

Address correspondence and reprint requests to Dr. Yeong-Min Park, Department of Immunology, Laboratory of Dendritic Cell Differentiation and Regulation, School of Medicine, Konkuk University, Chungju 380-701, South Korea. E-mail address: immun3023@kku.ac.kr

The online version of this article contains supplemental material.

Abbreviations used in this article: BCG, bacillus Calmette–Guérin; CCL19, chemokine ligand 19; DC, dendritic cell; E7-DC, DC pulsed with E7 peptide; HspX, heat shock protein X; HspX-E7-DC, HspX-treated DC pulsed with E7 peptide; IRF3, IFN response factor 3; LN, lymph node; MPLA, monophosphoryl lipid A; rm, recombinant mouse; TB, tuberculosis; TCF, transcription factor; TL, tumor lysate of B16-BL6.

This article is distributed under The American Association of Immunologists, Inc., [Reuse Terms and Conditions for Author Choice articles](#).

Copyright © 2014 by The American Association of Immunologists, Inc. 0022-1767/14/\$16.00

The 16-kDa HspX (Rv2031c) is required for mycobacterial persistence within the macrophage and is a dominant protein produced during static growth or under hypoxic conditions (8). The immunogenicity of HspX in BALB/c and C57BL/6 mice immunized with DNA plasmids encoding *hspX* was demonstrated by the induction of strong HspX Ag-specific Th1-type cytokine secretion and Ab production (9). In addition, IFN- $\gamma$  responses to HspX were significantly higher in *M. tuberculosis*-exposed individuals than in *M. tuberculosis*-unexposed BCG vaccinees (10). However, very little is known about how HspX elicits host immune responses. HspX is reported to be a promising candidate for TB vaccines owing to the induction of Th1-type T cell immunity. We believe that HspX boosts host immunity against *M. tuberculosis* by interacting with DCs as a TLR ligand. Thus, we speculate that HspX can ultimately be used as a key adjuvant in cancer therapeutic vaccination, especially in the context of DC-based immunotherapy.

In this article, we describe the biological activity and cellular immunity of *M. tuberculosis* HspX in DC-based CTL activation, as well as its potential as an adjuvant in DC-based antitumor immunotherapy. We show that HspX is a potent TLR4 agonist that can enhance both DC activation and Th1 polarization through the MyD88 and TRIF signaling pathways. Notably, HspX mediated a strong induction of Ag-specific CD8<sup>+</sup> T cell-mediated immune responses, leading to the regression of tumor growth and metastasis in vivo. These results open the door to promising possibilities for the use of HspX as a potential adjuvant for DC-based antitumor immunotherapies.

## Materials and Methods

### Mice

Male 6- to 8-wk-old C57BL/6 (H-2K<sup>b</sup> and I-A<sup>b</sup>) mice were purchased from the Korean Institute of Chemistry Technology (Orient, Daejeon, Korea). C57BL/6 OT-I and C57BL/6 OT-II TCR transgenic mice, C57BL/6J TLR2 knockout mice (*TLR2*<sup>-/-</sup>; B6.129-Tlr2<sup>tm1Ktir/J</sup>), C57BL/10 TLR4 knockout mice (*TLR4*<sup>-/-</sup>; C57BL/10ScNJ), MyD88 knockout mice, and TRIF-deficient mice aged 6–8 wk were purchased from The Jackson Laboratory (Bar Harbor, ME). They were housed in a specific pathogen-free environment within an animal facility for  $\geq 1$  wk before the experiment, and used in accordance with the institutional guidelines for animal care (Institutional Animal Care and Use Committee number: KU13047).

**Cell lines.** Primary C57BL/6 mouse lung epithelial cells were cotransformed with HPV-16 E6 and E7, and an activated ras oncogene to generate the TC-1 cells, as previously described (11). TC-1 cells were cultured in RPMI 1640 supplemented with 10% heat-inactivated FBS, 100 U/ml penicillin, 100  $\mu$ g/ml streptomycin, and 10 mM L-glutamine (all purchased from Invitrogen, Carlsbad, CA) at 37°C with 5% CO<sub>2</sub>.

### Reagents and Abs

Recombinant mouse GM-CSF, IL-4, CCL19, and the FITC-Annexin V/propidium iodine kit were purchased from R&D Systems (Minneapolis, MN). Dextran-FITC (40,000 Da) was purchased from Sigma-Aldrich (St. Louis, MO). LPS (from *Escherichia coli* O111:B4) was purchased from Invivogen (San Diego, CA). H-2K<sup>b</sup>-restricted OVA peptide (OVA<sub>257–264</sub>), H-2D<sup>b</sup>-restricted OVA peptide (OVA<sub>323–339</sub>), and HPV-16 E7 (aa 49–57) peptide (RAHYNIVTF) were synthesized by Peptron (Daejeon, Korea). The following FITC- or PE-conjugated mAbs were purchased from BD Biosciences (San Jose, CA): CD8 (SK17), CD11c (HL3), CD62L (MEL14), CD80 (16-10A1), CD83 (Michel-17), CD86 (GL1), Iab  $\beta$ -chain (AF-120.1), H-2K<sup>b</sup> (AF6-88.5), CCR7 (CD197), IL-10 (JESS-16E3), and IL-12p40/p70 (C15.6). Alexa 568-conjugated anti-mouse IgG Abs were purchased from Invitrogen (Eugene, OR). FITC-conjugated mouse IgG Abs and cytokine ELISA kits for murine IL-1 $\beta$ , IL-2, IL-6, IL-10, IL-12p70, TNF- $\alpha$ , IFN- $\beta$ , and IFN- $\gamma$  were purchased from eBiosciences (San Diego, CA).

### Expression and purification of recombinant HspX protein

The recombinant HspX protein was produced using the pET28a (Promega, Madison, WI) vector and *E. coli* expression system, as recently described (6). Briefly, *rv2301c* encoding HspX was amplified by PCR using *M. tu-*

*berculosis* H37Rv genomic DNA (ATCC 27294) as a template and the following primers: forward, 5'-GGG CCC GGA TCC ATG GCA AAG CTC TCC-3'; and reverse, 5'-GGG CCC GAA TTC CTT GAC GGT GAC GGT-3'. The PCR product was cut using BamHI and EcoRI, and then inserted into the pET28a vector, which was cut with the same restriction enzymes. The recombinant plasmid was transformed into *E. coli* BL21 cells carrying bacteriophage DE3 for protein overexpression.

**DC generation and culture.** DCs were generated from murine bone marrow cells according to the procedure of Inaba et al. (12), with minor modifications. In brief, bone marrow was flushed from the tibias and femurs of 6- to 8 wk-old male C57BL/6 mice and depleted of RBCs using RBC Lysing Buffer (Sigma-Aldrich). The cells were plated in six-well culture plates (1  $\times$  10<sup>6</sup> cells per milliliter; 3 ml per well) in RPMI 1640 supplemented with 10% heat-inactivated FBS, 100 U/ml penicillin, 100 mg/ml streptomycin, 20 ng/ml recombinant mouse (rm)GM-CSF, and 10 ng/ml rIL-4 at 37°C in 5% CO<sub>2</sub>. On days 3 and 5 of culturing, floating cells were gently removed and fresh medium was added. On day 6 of the culture, nonadherent cells and loosely adherent proliferating DC aggregates were harvested for analysis or stimulation. On day 7,  $\geq 90\%$  of the non-adherent cells expressed CD11c.

**Determination of affinity value of the binding of TLR4 and HspX.** The binding between rmTLR4/MD2 and HspX was performed using the BLITZ system (ForteBio, Menlo Park, CA). Human rTLR4/MD2 tagged with anti-penta-His (HIS) was purchased from R&D Systems (Minneapolis, MN). HIS biosensors (catalog no. 18-5078, ForteBio) were hydrated for 10 min prior to the experiment. The concentration of HIS-tagged rmTLR4/MD2 was 0.1 mg/ml, and that of both purified HspX and BSA, Pam3CSK4, and LPS was 2 mg/ml. The setting was as follows: initial baseline for 30 s, loading for 300 s, baseline for 60 s, association for 300 s, and dissociation for 300 s. The affinity value of HspX was generated by BLITZ pro software analysis as a nonadvanced kinetics experiment.

### Antigen uptake and migration of DCs

Ag uptake and in vitro and in vivo chemotaxis were performed as previously described (6).

**DC migration in vitro and in vivo.** DC migration was assayed by a modification of the Boyden chamber method (13) performed in a microchemotaxis chamber (NeuroProbe, Gaithersburg, MD) using a polycarbonate membrane (NeuroProbe) with a pore size of 5.0  $\mu$ m. The membranes were coated with mouse type IV collagen (20  $\mu$ g/ml in PBS) and placed between the chambers. First, the lower well of the chamber was filled with 27  $\mu$ l RPMI 1640 supplemented with 0.1% BSA following the addition of CCL19 at the indicated concentration. The DCs were washed with RPMI 1640 containing 0.1% BSA resuspended at a concentration of 1  $\times$  10<sup>6</sup> cells per milliliter in RPMI 1640 supplemented with 0.1% BSA. The cells were then placed in the upper well of the chamber (50  $\mu$ l per well) and incubated at 37°C in 95% air and 5% CO<sub>2</sub> for 2 h. At the end of the incubation, the filters were removed and all nonmigrated cells on the upper side of the filter were scraped off with wet tissue paper. The migrated cells on the other side of the filter were fixed for 2 min with fixative solution from the HEMA 3 stain set and stained with solutions 1 and 2 of the HEMA 3 stain set, each for 2 min (Fisher Scientific, Kalamazoo, MI). The numbers of stained cells were quantified densitometrically using IMAGE GAUGE Version 2.54 (Fujifilm) for data analysis. For the in vivo migration test, DCs were labeled with 0.5  $\mu$ M CFSE (Molecular Probes, Eugene, OR). Labeled cells (1  $\times$  10<sup>6</sup>) were injected s.c. in the hind-leg footpad. Popliteal lymph nodes (LNs) were removed 72 h later, mechanically disaggregated, and treated with collagenase A (1 mg/ml; Boehringer Mannheim, Indianapolis, IN) and DNase (0.4 mg/ml; Roche, Indianapolis, IN) for 30 min. The enzymatically treated cell suspension was evaluated for the number of CFSE<sup>+</sup> DCs by flow cytometry.

**MLR.** DCs were incubated with HspX or LPS in the presence or absence of OVA<sub>257–264</sub> (0.5  $\mu$ g/ml), OVA<sub>323–339</sub> (0.5  $\mu$ g/ml), or HPV 16-E7 peptide (1  $\mu$ g/ml) for 24 h. CFSE-labeled OT-I T cells (for OVA<sub>257–264</sub>), OT-II T cells (for OVA<sub>323–339</sub>), and naive T cells (for HPV 16-E7 peptide) were seeded in triplicate wells (1  $\times$  10<sup>5</sup> cells per well) in U-bottom, 96-well microtiter culture plates (Nunc), together with DCs (1  $\times$  10<sup>4</sup> cells per well). Cells were harvested after 96 h, stained with Cy5-labeled anti-CD8 and anti-CD4 mAb, and analyzed by flow cytometry (Becton Dickinson, San Jose, CA).

**Tumor protection assay.** Mice were s.c. injected with TC-1 (2  $\times$  10<sup>6</sup>) cells in the right lower back, followed by a footpad injection with PBS, DCs, or HspX-treated DCs (1  $\times$  10<sup>6</sup> cells per mouse) pulsed with or without HPV 16-E7 peptide (1  $\mu$ g/ml) on days 1, 3, and 5 after tumor inoculation. Groups of tumor-bearing mice were treated with PBS, DCs, DCs pulsed with E7 peptide (E7-DCs), or HspX-treated DCs pulsed with E7 peptide

(HspX-E7-DCs). Tumor size was measured every 2 d, and the tumor mass was calculated as  $V = (2A \times B)/2$ , where  $A$  is the length of the short axis and  $B$  is the length of the long axis.

**Lung metastasis assay.** Murine B16-BL6 melanoma cells were injected into the tail vein ( $3 \times 10^5$  cells per mouse). The hind leg footpads of the mice were then injected with PBS, DCs, or HspX-treated DCs ( $1 \times 10^6$  cells per  $50 \mu\text{l}$  per mouse) pulsed with or without H-2 Kb–restricted TRP2 peptide (aa 180–188,  $1 \mu\text{g}/\text{ml}$ ) on days 1, 3, and 7 of the posttumor injection. At 1 wk after the final immunization, the lungs were removed from these mice, and the metastatic nodules were quantified.

#### *In vivo CTL assay*

Mice were injected with PBS, DCs, DCs pulsed with E7-DCs, or HspX-E7-DCs on days 1 and 7. At 7 d after the last immunization, the splenocytes from the syngeneic mice were pulsed with or without HPV-16 E7 peptide ( $10 \mu\text{g}/\text{ml}$ ) for 45 min at  $37^\circ\text{C}$ . Then, the HPV-16 E7 peptide pulsed and unpulsed populations were loaded with either  $5 \mu\text{M}$  (high) or  $0.5 \mu\text{M}$  (low) CFSE (Molecular Probes) at  $37^\circ\text{C}$  for 10 min. The two populations were mixed 1:1 before tail vein injection into the immunized mice ( $10^7$  cells per mouse). At 4 h after the injection, the splenocytes were isolated, and the number of CFSE<sup>high</sup> and CFSE<sup>low</sup> populations was measured by flow cytometry.

#### *Statistical analysis*

Statistical significance was assessed by the Student paired  $t$  test. A  $p$  value  $< 0.05$  was considered statistically significant. Survival data were analyzed by the Kaplan–Meier log-rank test. Statistical analysis was conducted using Prism 4 GraphPad software (San Diego, CA).

## Results

### *HspX enhances the maturation of functional DCs*

HspX protein was carefully purified from soluble recombinant HspX (rRv2031) expressed in *E. coli* under endotoxin-free experimental conditions. However, we were concerned that the HspX may have been contaminated with endotoxin derived from the cell wall of *E. coli*, as it is a well-known factor of DC maturation. Therefore, we confirmed the purity and lack of endotoxin contamination of *E. coli*–derived HspX using the LAL endotoxin assay kit (GenScript USA) and immunoblot with the anti-histidine Ab. The levels of endotoxin in HspX were  $< 15 \text{ pg}/\text{ml}$  ( $< 0.1 \text{ EU}/\text{ml}$ ), and the molecular mass of purified HspX was  $\sim 16 \text{ kDa}$  (Supplemental Fig. 1A). In addition, proteinase K–treated or heat-treated HspX was unable to promote the production of secreted TNF- $\alpha$  and IL-6 in DCs. HspX was resistant to polymyxin B treatment, which is an inhibitor of LPS function (Supplemental Fig. 1B). We next investigated whether HspX affected DC viability and found that HspX-treated DCs showed no effect up to  $500 \text{ ng}/\text{ml}$  (Supplemental Fig. 1C).

After checking the safety of HspX in DCs, we measured the expression levels of surface molecules that are markers for DC maturation, including CD80, CD83, CD86, and MHC class I and II, on DCs following HspX stimulation. The upregulation of surface molecules on DCs following HspX stimulation occurred in a dose-dependent manner (Fig. 1A). Next, the levels of proinflammatory and anti-inflammatory cytokine secretion following stimulation of DCs with HspX were investigated. As shown in Fig. 1B, the levels of TNF- $\alpha$ , IL-6, IL-1 $\beta$ , and IFN $\beta$  were significantly induced in HspX-treated DCs (Fig. 1Ba). In addition, the levels of IL-12p70 in the HspX-treated DCs were significantly increased, whereas the levels of IL-10 were not altered. This finding indicates that HspX could be used as an adjuvant for the induction of a Th1 immune response (Fig. 1Bb). We reconfirmed the level of intracellular IL-12p70 and IL-10 production in HspX-treated DCs, and showed that IL-12p70<sup>+</sup> DCs increased only by HspX stimulation (Supplemental Fig. 2). In addition, the capacity of Ag (dextran) uptake, which decreases during DC maturation after Ag recognition, in HspX-treated DCs significantly decreased in a similar fashion to that observed in the LPS treatment (Fig. 1C). These

results indicate that HspX phenotypically and functionally activated DCs to promote Th1 immune responses.

### *HspX induces migration of DCs*

Because CCR7 is an important factor for the migration of DCs to lymphoid organs (14, 15), the increased levels of CCR7 expression in HspX-treated DCs were confirmed (Fig. 2A). We also used an *in vitro* Transwell migration assay to analyze the DC migratory capacity in response to chemokine ligand 19 (CCL19), which is the ligand for CCR7. An increase in the migration of DCs was observed in the HspX-treated DCs (Fig. 2B), which is consistent with the upregulation of CCR7 expression.

To further confirm the migratory capacity of DCs in response to HspX stimulation, we investigated the number of CFSE<sup>+</sup> DCs in the draining LNs *in vivo*. The number of CFSE<sup>+</sup> DCs in the draining LNs was significantly increased in the HspX-treated groups compared with those without HspX treatment (Fig. 2C). Therefore, these results demonstrate that HspX promotes DC migration *in vitro* and *in vivo*, and suggest that the Ag-specific T cell response is enhanced in HspX-treated DCs.

### *HspX enhances the maturation of functional DCs via a TLR4-dependent pathway*

Next, using TLR2<sup>-/-</sup> and TLR4<sup>-/-</sup> mice, we investigated which TLRs are crucial in HspX-mediated maturation of DCs. The expression of surface molecules (CD86 and MHC class II) was enhanced in HspX-treated WT and TLR2<sup>-/-</sup> DCs, whereas these effects were significantly abrogated in TLR4<sup>-/-</sup> DCs (Fig. 3A). Of interest, neither HspX nor LPS (a TLR4 agonist) enhanced the secretion of proinflammatory cytokines (TNF- $\alpha$ , IL-6, and IL-1 $\beta$ ) in DCs from TLR4<sup>-/-</sup> mice. These results indicate that TLR4 mediation is critical for DC maturation by HspX (Fig. 3B).

Furthermore, to determine whether HspX directly bound to TLR4, we measured the direct binding of TLR4 with HspX using the BLItz system. HIS-tagged recombinant TLR4/MD2 was labeled with an anti-penta-HIS biosensor. After washing away the loosely bound TLR4/MD2, association was initiated by dipping the TLR4-tagged HIS biosensor in solutions of BSA (negative control), Pam3CSK4, LPS, HspX, or PBS, and then monitored in real time. Dissociation was initiated by dipping the same biosensor into PBS and was then monitored in the same manner. The calculated values of  $K_a$ ,  $K_d$ , and  $K_D$  between HspX and TLR4 were  $6.677 \times 10^5$  (1/Ms),  $3.433 \times 10^{-3}$  (1/S), and  $5.14 \times 10^{-9}$  (M), respectively (Fig. 3C). Comparatively, BSA (a non-TLR agonist) and Pam3CSK4 (a TLR2 agonist) did not bind TLR4. These results indicate that HspX has a strong binding affinity to TLR4/MD2.

### *The MyD88 and TRIF signaling pathways are involved in HspX-induced maturation of DCs*

Toll/IL-1 receptor domain–containing adaptors such as MyD88 and TRIF are key modulators in TLR4-mediated intracellular signaling pathways. To investigate the involvement of the MyD88 and TRIF signaling pathways in the production of proinflammatory cytokines, we measured proinflammatory cytokine production in DCs derived from WT, MyD88<sup>-/-</sup> mice, or TRIF-deficient mice exposed to HspX or LPS. The production of TNF- $\alpha$ , IL-1 $\beta$ , and IL-6 in both the HspX-treated DCs and LPS-treated DCs was significantly diminished in the absence of MyD88 or TRIF (Fig. 4A).

Among the earliest events following TLR4 ligation is its association with the adaptor proteins MyD88 and TRIF, both of which initiate distinct signaling pathways (16). To confirm whether HspX directly activated TLR4 and the downstream TLR4 signals, we

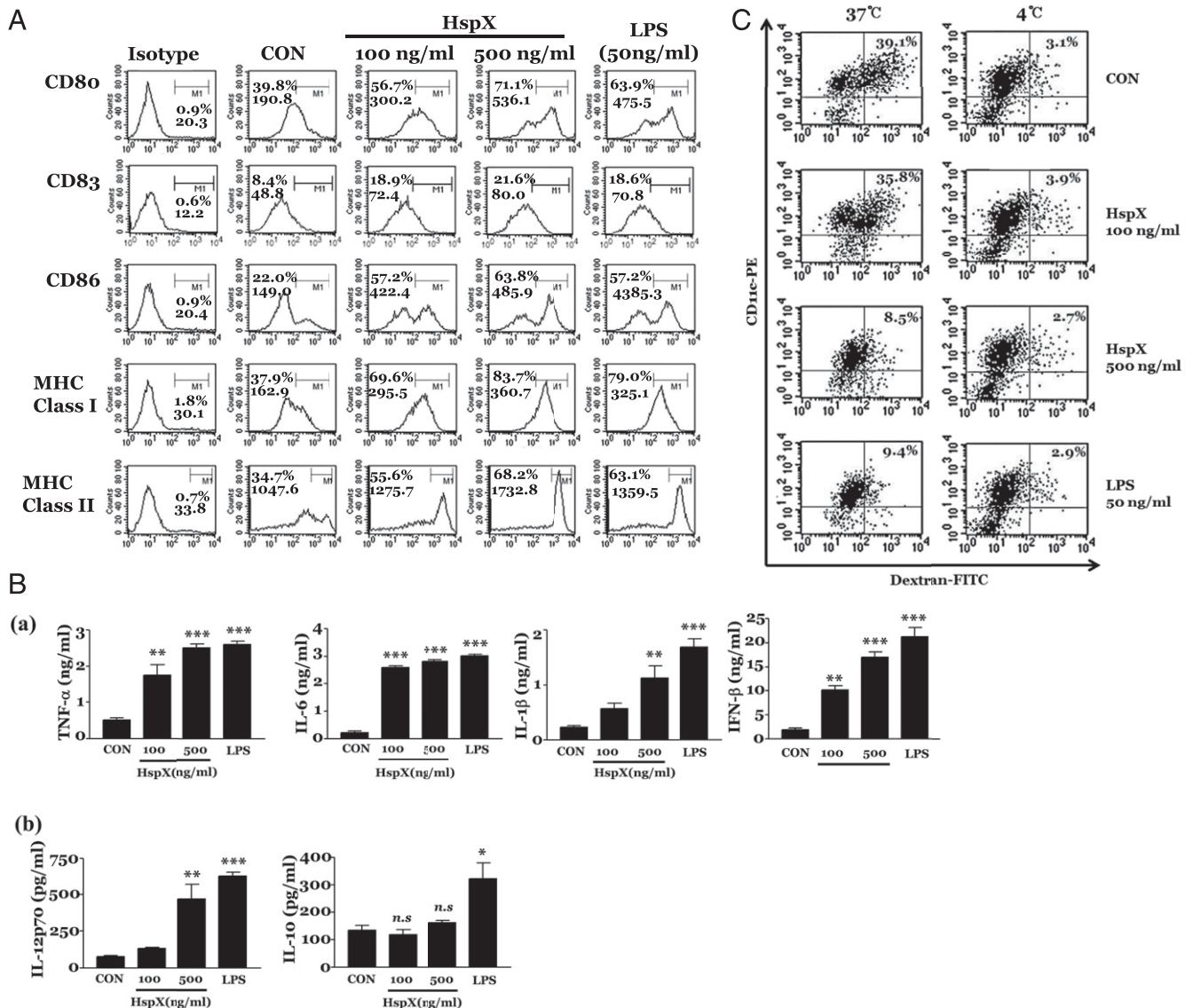


**FIGURE 1.** HspX enhances the phenotypical and functional maturation of DCs. **(A)** DCs were treated with the indicated concentrations of HspX or LPS for 24 h. Flow cytometry was used to analyze the expression of surface molecules on the CD11c<sup>+</sup> cells. The mean fluorescence intensity and the percentage of positive cells are shown in each panel. The results of one representative experiment ( $n = 5$ ) are shown. **(B)** DCs were treated with the indicated concentrations of HspX or LPS (50 ng/ml) for 24 h. ELISAs were performed to test the IL-12p70, IL-10, TNF- $\alpha$ , IL-6, IL-1 $\beta$ , and IFN- $\beta$  production in HspX-treated and LPS-treated DCs. Data are the mean and SEM ( $n = 3$ ). \* $p < 0.05$ , \*\* $p < 0.01$ , \*\*\* $p < 0.001$  compared with untreated DCs (CON) (**Ba** and **Bb**). **(C)** Endocytic activity of HspX-treated versus untreated DCs (CON). Endocytic activity at 37°C or 4°C was assessed by flow cytometry analysis as dextran-FITC uptake. The percentages of dextran-FITC<sup>+</sup>CD11c<sup>+</sup> cells are shown. The results of one representative experiment ( $n = 5$ ) are shown.

performed an immunoprecipitation assay and a Western blot assay. HspX activated the tyrosine phosphorylation of TLR4 (Fig. 4Ba) and then enhanced the interaction of MyD88 and IRAK4 (Fig. 4Bb). In addition, HspX activated the phosphorylation of IFN response factor 3 (IRF3), which is a transcription factor for the induction of IFN- $\beta$  in the TRIF-mediated signaling cascade (Fig. 4Bc).

Furthermore, we investigated three downstream pathways of MyD88, namely, MAPKs, NF- $\kappa$ B, and PI3K/PDK1/Akt (17) (18), which promote TLR4-mediated proinflammatory cytokine production in DCs stimulated by HspX. We found that HspX enhanced the phosphorylation of MAPKs such as ERK, JNK, and p38MAPK (Fig. 4C), activated NF- $\kappa$ B regulated by IKK $\alpha$ / $\beta$  and I $\kappa$ B $\alpha$  (Fig. 4D), and enhanced TLR4-mediated PDK1 and Akt phosphorylation (Fig. 4E). Taken together, these findings suggest that TLR4-mediated MyD88-dependent and TRIF-dependent pathways are crucial for optimal HspX-induced DC activation.

#### HspX enhances naive T cell proliferation and Th1 polarization via DC activation

The major roles of mature DCs are Ag presentation, interaction with T cells, and subsequent T cell activation. To clarify the effect of HspX on DC and T cell interactions, we performed a syngeneic MLR assay using OT-I TCR transgenic CD8<sup>+</sup> T cells and OT-II TCR transgenic CD4<sup>+</sup> T cells (19). The CFSE-labeled OVA-specific CD4<sup>+</sup> and CD8<sup>+</sup> T cells proliferated in and cocultured with DCs presenting OVA<sub>257–264</sub> (Fig. 5Aa) or OVA<sub>323–339</sub> (Fig. 5Ab), which was significantly potentiated by HspX treatment (Fig. 5A). Furthermore, the production of IFN- $\gamma$  by the activated T cells was also significantly enhanced by HspX (Fig. 5B). Combining these results with the IL-12p70 production of DCs (Fig. 1Bb), we propose that HspX-treated DCs could be used in cancer immunotherapy to polarize naive CD4<sup>+</sup> and CD8<sup>+</sup> T cells toward an IFN- $\gamma$ -producing Th1-type T cell phenotype.

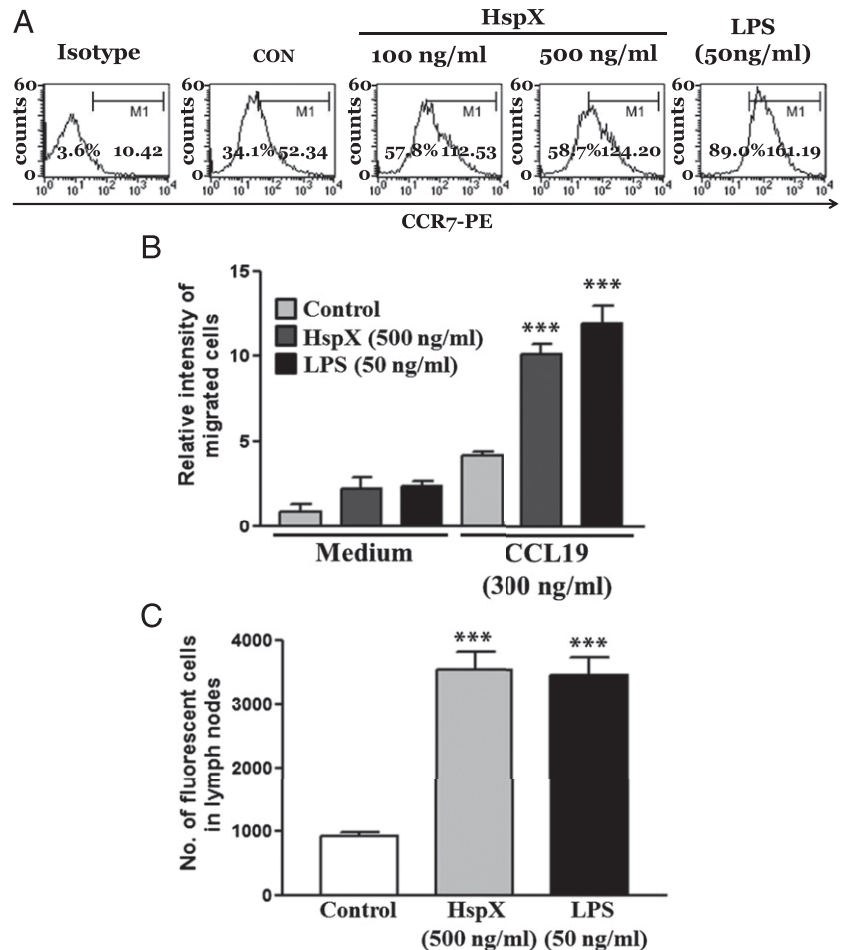


**FIGURE 2.** HspX enhances the migration of DCs in vitro and in vivo. **(A)** DCs were treated with the indicated concentrations of HspX or LPS for 24 h. The percentage of CCR7<sup>+</sup>CD11c<sup>+</sup> DCs was analyzed by flow cytometry. The number in each panel indicates the percentage of positive cells. A representative experiment ( $n = 5$ ) is shown. **(B)** DCs were treated with HspX or LPS for 24 h and then subjected to an in vitro Transwell chemotaxis assay in which movement toward medium alone or medium containing CCL19 (300 ng/ml) was measured. **(C)** CFSE-labeled HspX-treated or LPS-treated DCs were s.c. injected into the hind leg footpad of mice, and the cells were recovered from popliteal LNs 72 h later and analyzed. \*\*\* $p < 0.001$  compared with untreated DCs (control).

We performed a syngeneic MLR assay using cervical tumor-specific Ag E7 peptide to check whether HspX has immunoadjuvanticity in cancer vaccination against virtual cervical cancer. Although CFSE-labeled CD8<sup>+</sup> (Fig. 5Aa) or CD4<sup>+</sup> (Fig. 5Ab) T cells proliferated in coculture with DCs presenting E7 peptide, these T cells also significantly proliferated in HspX-treated DCs (Fig. 5C). IFN- $\gamma$  production by activated T cells was also significantly enhanced by HspX treatment (Fig. 5D). We next analyzed the differentiation of CD4 T cells by HspX-activated DCs, measuring through the intracellular cytokine staining and transcription factor (TCF) staining. As shown in Fig. 6, we investigated whether HspX-treated DCs increased the levels of a Th1-type cytokine, IFN- $\gamma$ , and a Th1-type transcriptional factor, T-bet; however, Th2- and Th17-type cytokines, IL-4 and IL-17A, and GATA-3 (TCF for Th2) and RoR $\gamma$ t (TCF for Th17) did not. In summary, DCs activated by HspX elevate the proliferation of CD4<sup>+</sup> and CD8<sup>+</sup> T cells and differentiate CD4<sup>+</sup> T cells toward Th1 immunity.

#### *HspX enhances the efficacy of DC-based antitumor immunotherapy against a cervical cancer model*

The above results of enhanced tumor Ag (E7)-specific T cell proliferation by HspX (Fig. 5C, 5D) motivated us to test the effect of HspX on DC immunotherapy in an in vivo model of cervical cancer. Injection of E7-DCs significantly inhibited TC-1 tumor growth compared with mice receiving PBS or immature DCs (Fig. 7A). Of interest, injection of HspX-E7-DCs reduced the TC-1 tumor growth further than that achieved by E7-DC injections (Fig. 7A). Notably, >60% of the mice injected with the HspX-E7-DCs survived beyond 60 d following the TC-1 tumor implantation, whereas only 20% of the mice injected with E7-DCs survived

during the same period. All the mice in the PBS and DC-injected groups died within 46 d after tumor implantation (Fig. 7B).

To assess whether activated CD8<sup>+</sup> T cells among splenocytes in the tumor model were enhanced by HspX-E7-DCs, we measured the surface expression levels of CD62L and CD44, which promote CD8<sup>+</sup> T cell migration to the site of Ag deposition (6). Although the number of activated CD8<sup>+</sup> T cells (CD62L<sup>low</sup>CD44<sup>high</sup>) from the mice injected with E7-DCs (21% of CD44 and 34% of CD62L) was enhanced compared with that of mice injected with either PBS (5% of CD44 and 54% of CD62L) or DCs (7% of CD44 and 51% of CD62L), the number of activated CD8<sup>+</sup> T cells from mice injected with HspX-E7-DCs (32% of CD44 and 15% of CD62L) was significantly higher than that of mice injected with E7-DCs (Fig. 7C).

Finally, we determined the ability of activated CD8<sup>+</sup> T cells stimulated by HspX-E7-DCs to kill tumor cells using an in vivo CTL activity assay. We found that a significantly high level of target cell lysis was observed in mice that received HspX-E7-DCs ( $54.2 \pm 0.35\%$ ) compared with those that received PBS ( $0 \pm 0.05\%$ ), DCs ( $0.1 \pm 0.04\%$ ), or E7-DCs ( $22.3 \pm 0.28\%$ ) (Fig. 7D). These results indicate that HspX could be a crucial factor for cancer vaccine against E7<sup>+</sup> cervical tumor by enhancing killing activity to target cells.

#### *HspX enhances the efficacy of DC-based antitumor immunotherapy against the B16-BL6 pulmonary metastasis model*

Tumor immunotherapy using DC vaccination was expected to be effective in the prevention of metastasis and recurrence of the primary tumor, as well as in regression of the primary tumor mass. Therefore, we determined whether HspX-treated DCs pulsed with

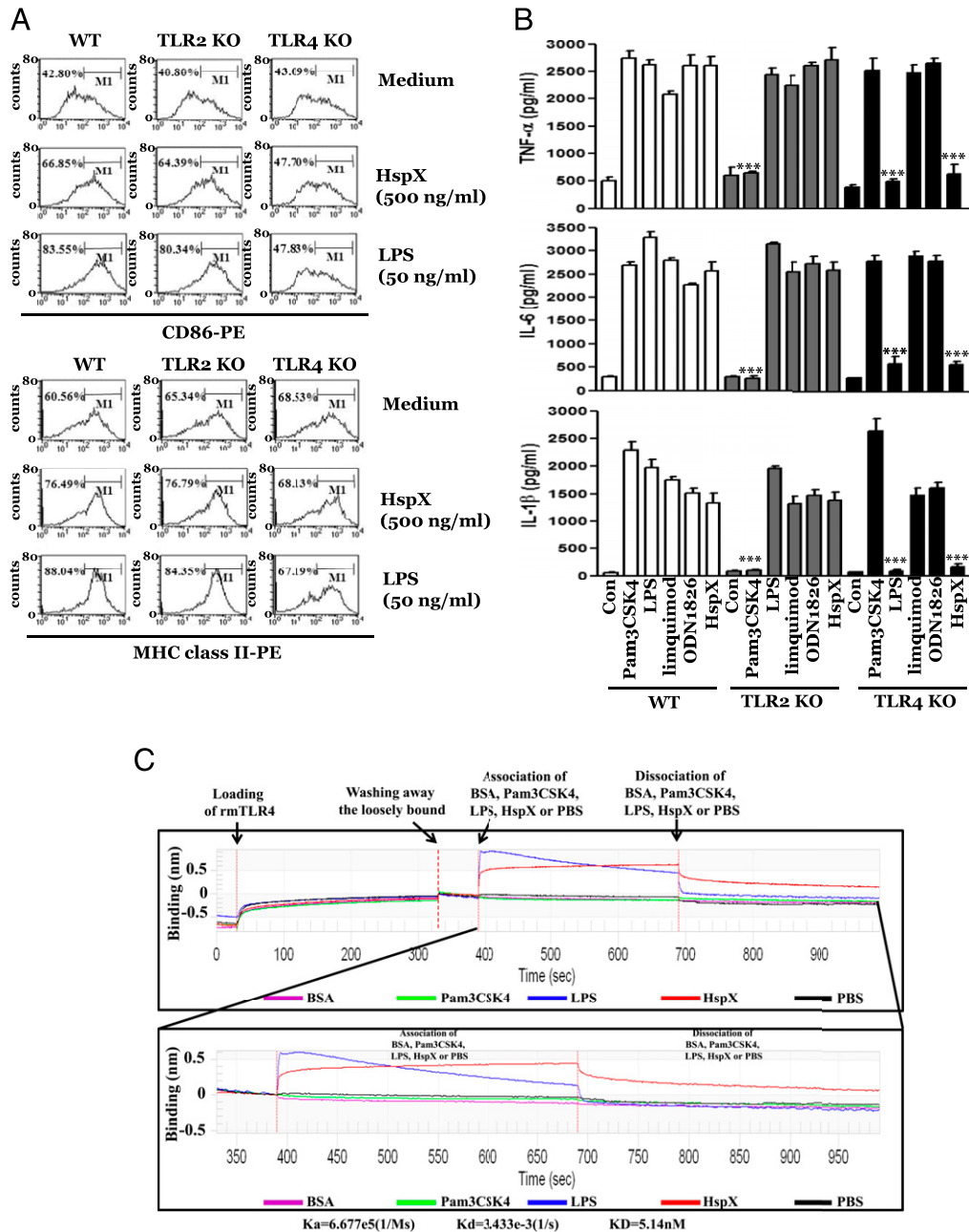


**FIGURE 3.** HspX induces the phenotypical and functional maturation of DCs by binding to TLR4. **(A)** DCs derived from WT, TLR2<sup>-/-</sup>, and TLR4<sup>-/-</sup> mice were treated with HspX (500 ng/ml) or LPS (50 ng/ml) for 24 h. Flow cytometry was used to analyze the expression of the surface molecules CD86 and MHC class II on the CD11c<sup>+</sup> cells. The percentage of positive cells is shown in each panel. The results of one representative experiment ( $n = 5$ ) are shown. **(B)** DCs derived from WT, TLR2<sup>-/-</sup>, and TLR4<sup>-/-</sup> mice were treated with Pam3CSK4 (TLR2 agonist, 10  $\mu$ g/ml), LPS (TLR4 agonist, 50 ng/ml), imiquimod (TLR7 agonist, 1  $\mu$ g/ml), ODN1826 (TLR9 agonist, 10  $\mu$ g/ml), or HspX (500 ng/ml) for 24 h. ELISAs were performed to test TNF- $\alpha$ , IL-6, and IL-1 $\beta$  production in HspX agonist-treated or TLRs agonist-treated DCs. Data are mean and SEM ( $n = 3$ ). \*\*\* $p < 0.001$  compared with WT cultures. **(C)** The BLITZ system results for the interaction of rmTLR4/MD2 with HspX (red line), positive control (LPS = blue line), and negative control (BSA = purple line, Pam3CSK4 = green line, or PBS = black line) are shown. The vertical and horizontal axes represent the light shift distance (nm) and association/dissociation time (sec), respectively. The affinity value,  $K_D$ , was calculated from the association and dissociation curves of HspX.

tumor lysate of B16-BL6 (TL) and TRP2, which is a tumor-associated Ag of B16-BL6, have anti-B16-BL6 pulmonary metastasis effects, using a therapeutic protocol. B16-BL6 metastatic nodules in the lungs were reduced by immunization with TL-pulsed DCs (Fig. 8A) or TRP2 peptide-pulsed DCs (Fig. 8B). They were further reduced by immunization with TL-pulsed HspX-treated DCs or TRP2 peptide-pulsed HspX-treated DCs (Fig. 8). These data indicate that HspX-treated DCs have an inhibitory effect on B16-BL6 pulmonary metastasis.

## Discussion

In this study, we focused on *M. tuberculosis* HspX, which has been used as an effective adjuvant for BCG vaccination (20). The finding that it potentiated the CTL immune response in TB vaccination supports its application in cancer vaccinations. We found that HspX was a highly selective agonist of TLR4 in DCs. HspX strongly bound to TLR4 in the BLITZ assay and activated the TLR4 signaling pathway. This study also showed enhanced expression of CD86 and MHC class II and the production of

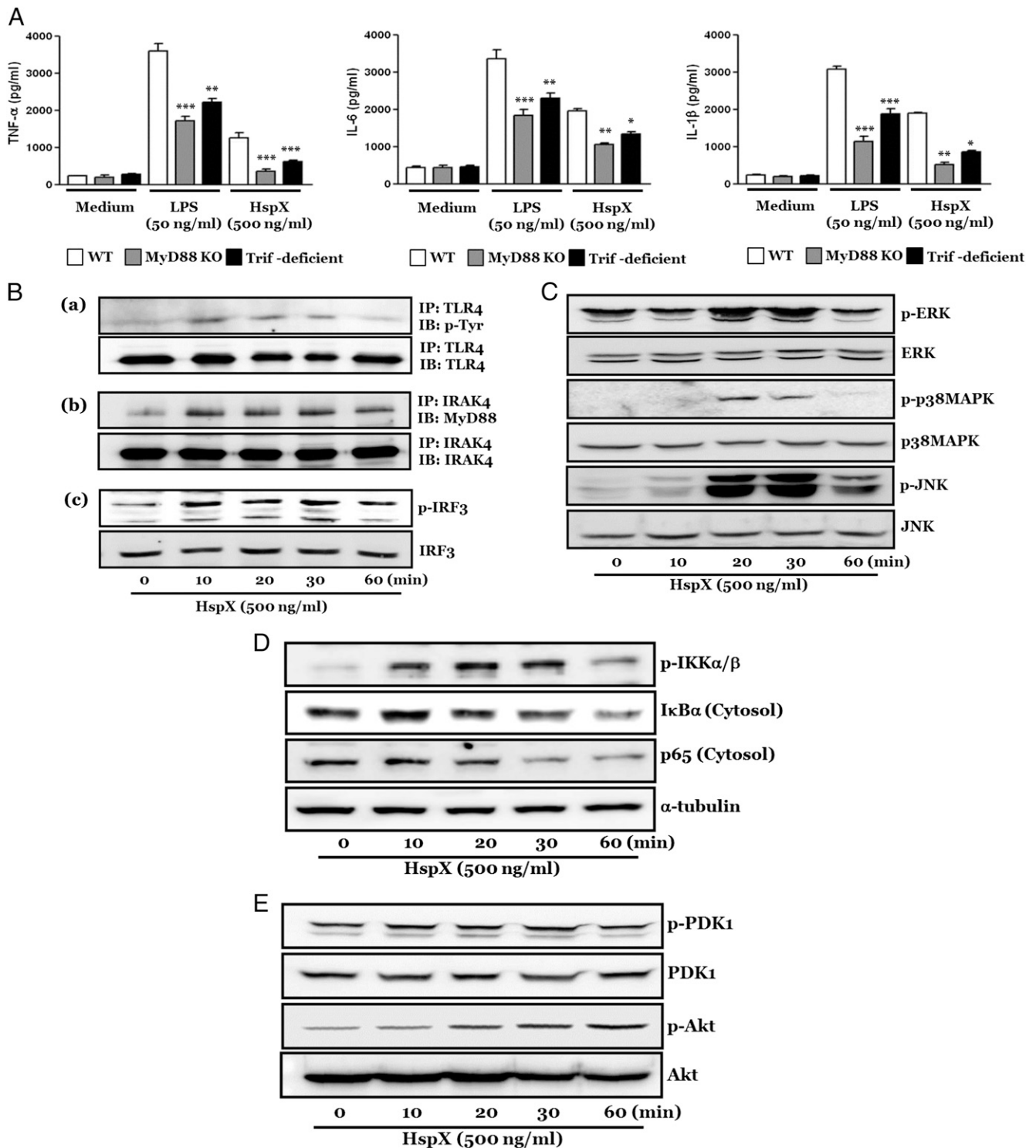


**FIGURE 4.** HspX-induced cytokine production is mediated by both the MyD88 and TRIF pathways. **(A)** DCs derived from WT, MyD88<sup>-/-</sup>, and TRIF-deficient mice were treated with the indicated concentrations of HspX or LPS for 24 h. The supernatants were harvested and ELISAs were performed to test TNF-α, IL-6, and IL-1β production. Data are the mean and SEM (*n* = 3). \**p* < 0.05, \*\**p* < 0.01, \*\*\**p* < 0.001 compared with WT cultures. **(B)** DCs were treated with HspX (500 ng/ml) at the indicated time points. The cells were harvested, and the cell lysates (1 mg) were immunoprecipitated with anti-TLR4. The immunoprecipitated proteins were visualized by immunoblot with anti-p-Tyr or anti-TLR4 Abs **(a)**. The cells were harvested, and the cell lysates (1 mg) were immunoprecipitated with anti-IRAK4. The immunoprecipitated proteins were visualized by immunoblot with anti-MyD88 or anti-IRAK4 Abs **(b)**. The cells were harvested, and the cell lysates were visualized by immunoblot with anti-p-IRF3 or anti-IRF3 Abs **(c)**. **(C)** DCs were treated with HspX (500 ng/ml) at the indicated time points. The cells were harvested, and the cell lysates were visualized by immunoblot with anti-p-ERK, anti-ERK, anti-p-p38MAPK, anti-p38MAPK, anti-p-JNK, or anti-JNK Abs. **(D)** DCs were treated with HspX (500 ng/ml) at the indicated time points. The cells were harvested, and the cell lysates were visualized by immunoblot with anti-p-IKKα/β, anti-IκBα, anti-p65, or anti-α-tubulin Abs. **(E)** DCs were treated with HspX (500 ng/ml) at the indicated time points. The cells were harvested, and the cell lysates were visualized by immunoblot with anti-p-PDK1, anti-PDK1, anti-p-Akt, or anti-Akt Abs.

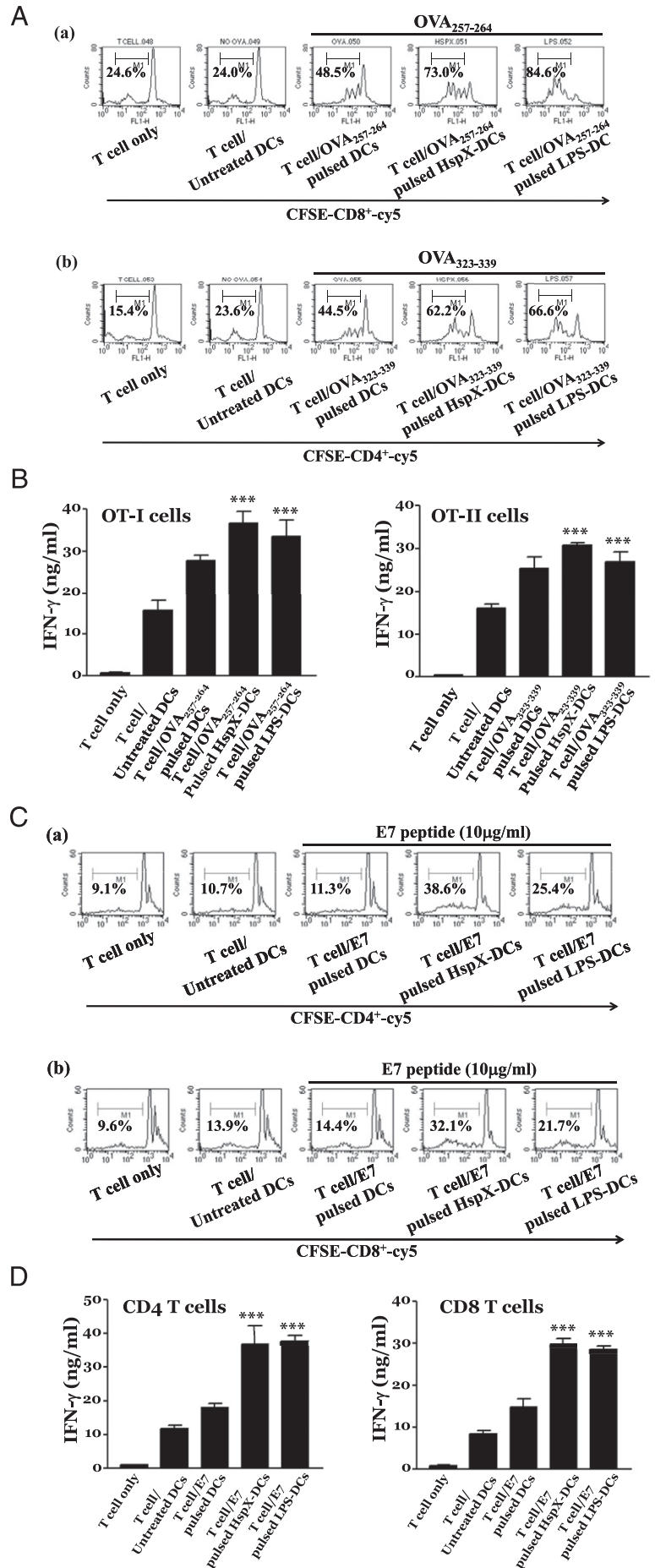


**FIGURE 5.** HspX-treated DCs induce proliferation of CD4<sup>+</sup> and CD8<sup>+</sup> T cells and a Th1 response. **(A)** Transgenic OVA-specific CD8<sup>+</sup> T cells **(a)** and OVA-specific CD4<sup>+</sup> T cells **(b)** were isolated and stained with CFSE and cocultured for 96 h with untreated DCs, DCs pulsed with OVA<sub>257-264</sub>, HspX (500 ng/ml)-treated DCs pulsed with OVA<sub>257-264</sub>, or LPS (50 ng/ml)-treated DCs pulsed with OVA<sub>257-264</sub>. T cell proliferation was assessed by flow cytometry, and the percentage of proliferating cells is shown in each panel. A representative experiment ( $n = 3$ ) is shown. **(B)** At 24 h after culture, IFN- $\gamma$  production was measured in the supernatant by ELISA. \*\*\* $p < 0.001$  compared with the value from T cell/OVA peptide-pulsed DCs. **(C)** T cells were isolated and stained with CFSE, cocultured for 96 h with untreated DCs, DCs pulsed with E7 peptide, HspX (500 ng/ml)-treated DCs pulsed with E7 peptide, or LPS (50 ng/ml)-treated DCs pulsed with E7 peptide, and then stained with anti-PE/Cy5-conjugated CD4 or CD8 Abs. T cell proliferation was assessed by flow cytometry, and the percentage of proliferating cells is shown in each panel. A representative experiment ( $n = 3$ ) is shown. **(D)** At 24 h after culture, IFN- $\gamma$  production was measured in the supernatants by ELISA. \*\*\* $p < 0.001$  compared with the value from T cell/E7 peptide-pulsed DCs.

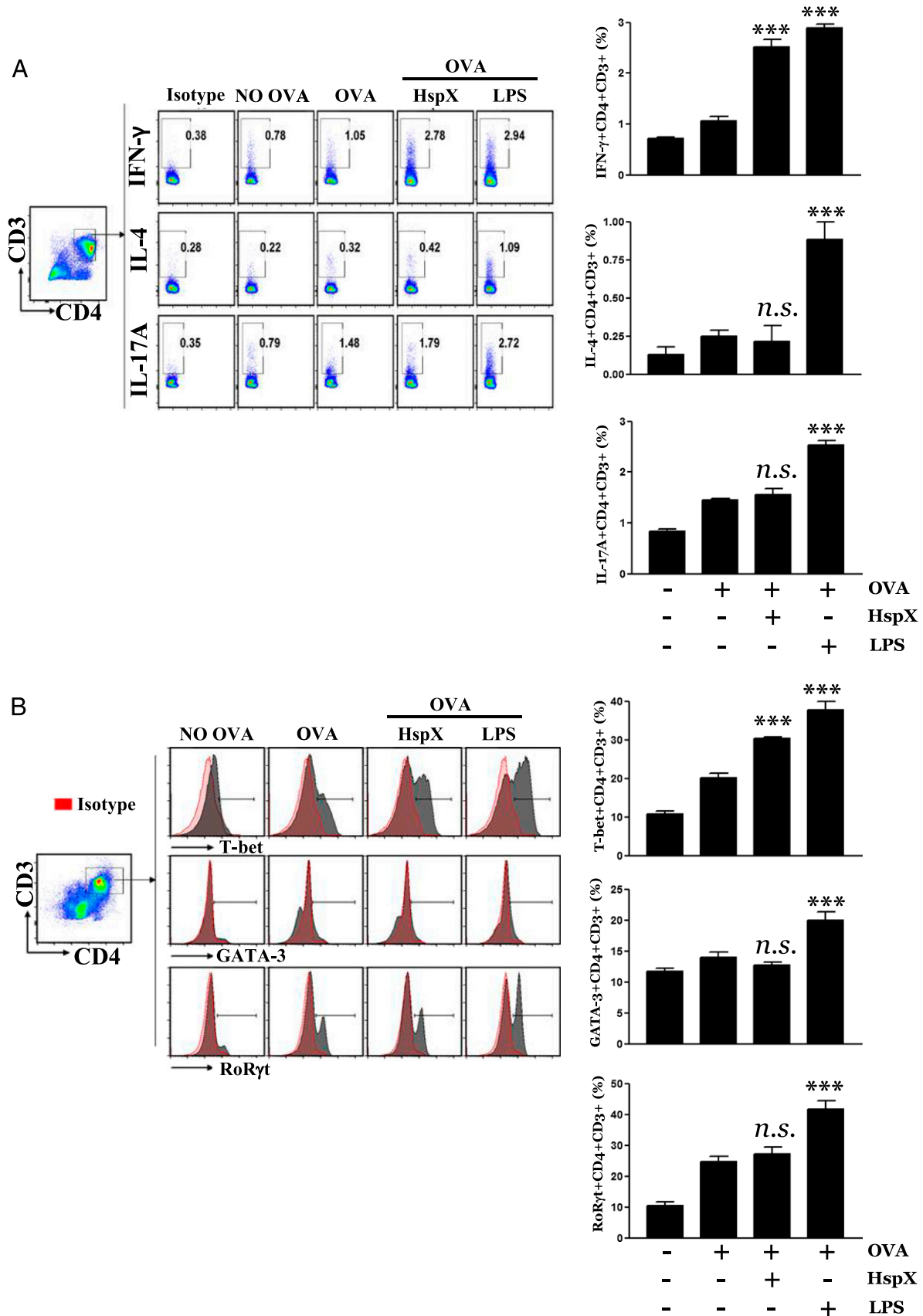


**FIGURE 6.** HspX-treated DCs stimulate T cells to Th1, but not Th2 or Th17. Transgenic OVA-specific CD4<sup>+</sup> T cells were isolated and cocultured for 72 h with DCs treated with HspX (500 ng/ml) or LPS (50 ng/ml), then pulsed with OVA<sub>323-339</sub> (1  $\mu$ g/ml) to produce OVA-specific CD4<sup>+</sup> T cells. T cells alone and T cells cocultured with untreated DCs served as controls. The graphs show intracellular cytokine production (**A**) and transcription factors (**B**) in CD3<sup>+</sup>/CD4<sup>+</sup>. (A) IFN- $\gamma$ , IL-4, or IL-17A expression in CD3<sup>+</sup>/CD4<sup>+</sup> was analyzed in T cells. (B) T-bet, GATA-3, and ROR $\gamma$ t expression in CD3<sup>+</sup>/CD4<sup>+</sup> cells was assessed by intracellular staining. \*\*\**p* < 0.001 compared with the value from OVA group.

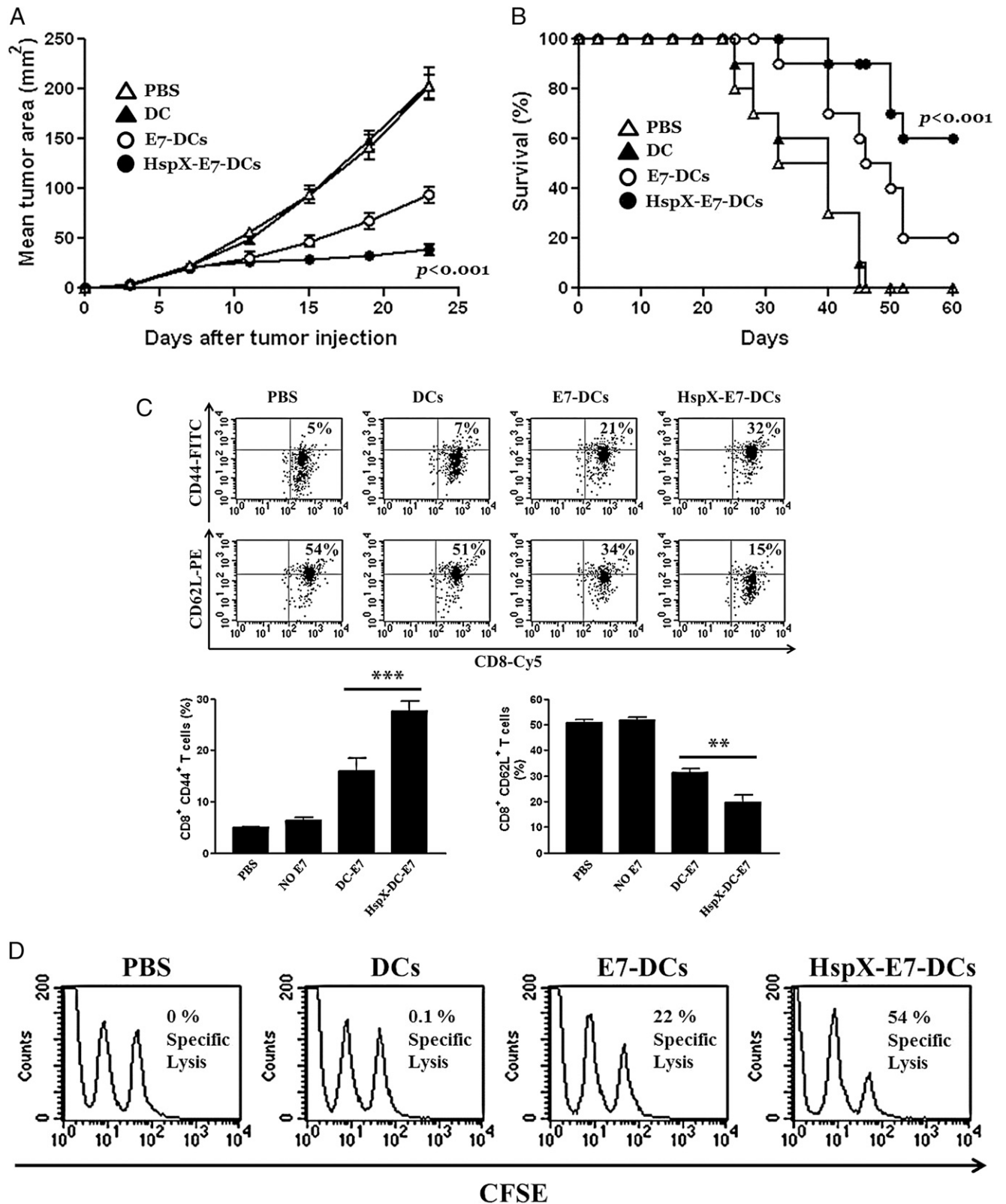


**FIGURE 7.** HspX-treated DCs pulsed with HPV 16-E7 protects mice against TC-1 tumor challenge. Mice were s.c. challenged with  $3 \times 10^5$  TC-1 tumor cells into the right flank area. For administration of DCs ( $1 \times 10^6$  cells/mouse), mice were i.v. injected with PBS, DCs, E7-DCs, or HspX-E7-DCs on days 1, 3, and 5 after the tumor challenge. **(A)** Following tumor challenge with TC-1 cells, tumor growth was monitored by measuring the diameter every 2 d. *p* < 0.001, HspX-E7-DCs versus E7-DCs groups (*n* = 10 per group). **(B)** Survival of mice with TC-1 tumor challenge after injection of PBS, DCs, E7-DCs, or HspX-E7-DCs (*n* = 10 mice per group). The *p* value was calculated by the Kaplan–Meier log-rank test between two groups of mice injected with E7-DCs and HspX-E7-DCs. **(C)** On day 20 post challenge with TC-1 tumor cells, splenocytes were isolated and analyzed for the expression of CD62L and CD44 on CD8<sup>+</sup> T cells. The percentage of positive cells is shown for each panel. Bar graphs show the mean percentage  $\pm$  SEM of CD62L<sup>+</sup> and CD44<sup>+</sup> on CD8<sup>+</sup> T cells (*n* = 3). \*\**p* < 0.05, \*\*\**p* < 0.001. **(D)** In vivo CTL activity. C57BL/6 mice were primed with PBS, immature DCs, E7-DCs, (Figure legend continues)

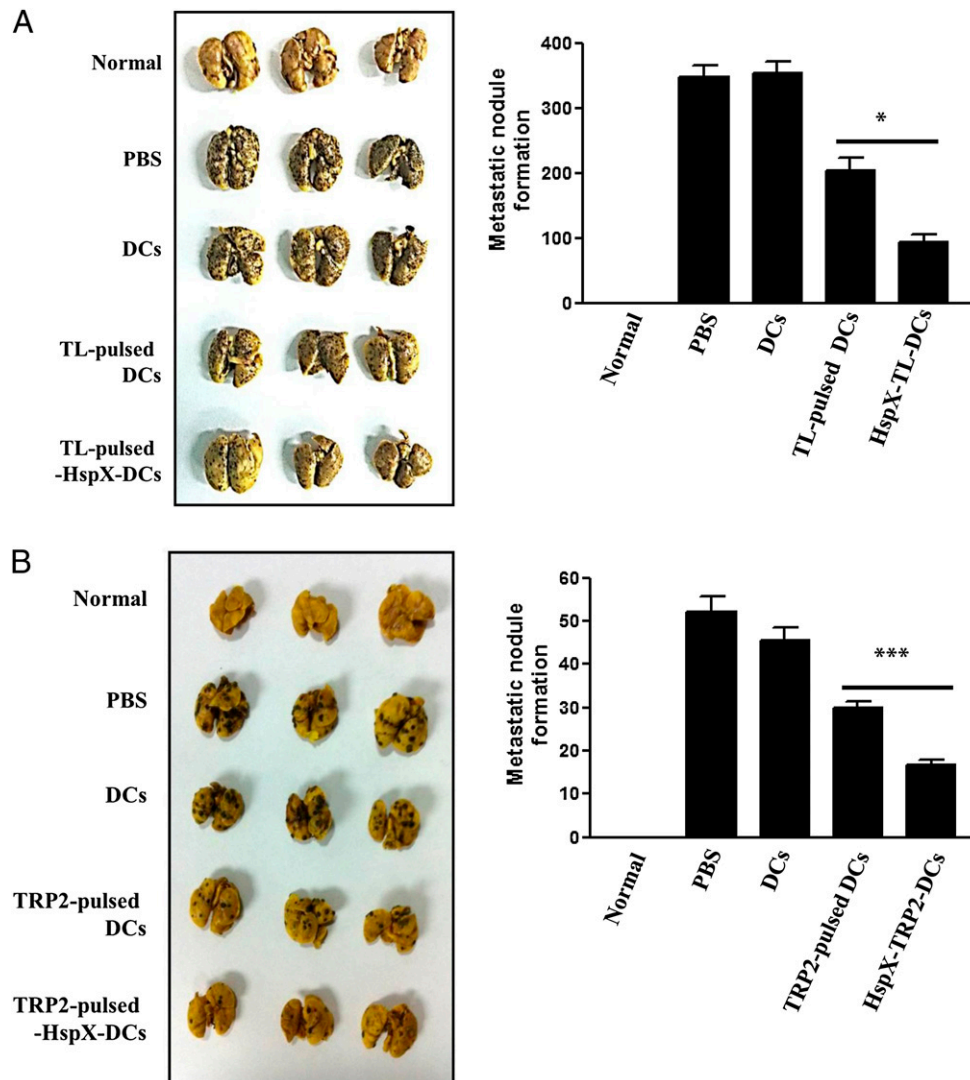


**FIGURE 8.** HspX-treated DCs pulsed with HPV 16-E7 inhibit B16-BL6 pulmonary metastasis. Mice were i.v. challenged with  $3 \times 10^5$  B16-BL6 melanoma tumor cells. **(A)** For administration of DCs ( $1 \times 10^6$  cells per mouse), mice were s.c. injected into their hind leg footpad with PBS, DCs, TL-pulsed DCs, or HspX-treated DCs pulsed with TL (HspX-TL-DCs) on days 1, 3, and 7 after tumor challenge. **(B)** For administration of DCs ( $1 \times 10^6$  cells per mouse), mice were s.c. injected into their hind leg footpad with PBS, DCs, DCs pulsed with TRP2 peptide (TRP2-DCs), or HspX-treated DCs pulsed with TRP2 peptide (HspX-TRP2-DCs) on days 1, 3, and 7 after the tumor challenge. At 1 wk after the final immunization, the metastatic nodules in their lungs were counted. Bar graphs show the mean  $\pm$  SEM of the formation number of metastatic nodules from 10 mice. \* $p < 0.05$ , \*\*\* $p < 0.001$ .

proinflammatory cytokines such as TNF- $\alpha$ , IL-6, and IL-1 in DCs as a result of the MyD88-dependent and TRIF-dependent pathways. We proved that MyD88 activated MAPKs, NF- $\kappa$ B, and PI3K/PDK1/Akt pathways through adaptation with IRAK4. In addition, phosphorylation of IRF3, a well-known downstream molecule of TRIF, showed an increase in HspX-treated DCs. Our results suggest that both intracellular adapters, namely, MyD88 and TRIF, are involved in mediating proinflammatory cytokine production in HspX-treated DCs.

To test the adjuvant effect of HspX, we performed in vivo CTL assays using the HPV-16 E7 Ag. This Ag is functionally required for the initiation and maintenance of both precursor and invasive lesions in cervical cancer (21). The percentage of target cell lysis in mice that received HspX-E7-DCs (54%) was significantly higher than that in mice that received PBS (0%), DCs (0.1%), or

E7-DCs (22%). Similar to the in vivo CTL activities that used the HPV-16 E7 peptide, systemic administration of HspX-E7-DCs induced a remarkable suppression of tumor growth. Using the same model, we observed that the antitumor activity of HspX originated from the marked increase in IFN- $\gamma$  production in the T cells primed by DCs stimulated with HspX in the draining LNs. We also noted an increase in the number of functional Ag-specific CTLs, and increased numbers of activated CD8<sup>+</sup> T cells (CD62L<sup>low</sup> CD44<sup>high</sup>). Therefore, HspX influenced the function of DCs in multiple ways, and we suggest that it is an effective adjuvant for DC-based antitumor immunotherapy against cervical cancer.

We examined whether the tumor-killing effect of CD8<sup>+</sup> T cells activated by HspX-E7-DCs also occurred in vivo using the CTL activity assay. CTLs from mice injected with E7-DCs efficiently lysed E7-pulsed splenocytes (target cells); however, CTLs from

or HspX-E7-DCs on days 1 and 7. At 7 d after boosting, CTL activity was determined by challenge with CFSE<sup>high</sup> E7 peptide-loaded splenocytes. Number indicates the percentage of specific killing. A representative experiment ( $n = 4$ ) is shown.

mice injected with PBS or DCs could not efficiently lyse the target cells (Figure 6D). In addition, CTLs from mice injected with HspX-E7-DCs were able to lyse a significantly higher number of target cells than the CTLs from mice injected with E7-DCs (Figure 6D). These results indicate that DCs activated by HspX could induce an antitumor immune response via activating CD8<sup>+</sup> T cell-mediated cytotoxic activity against cervical tumors.

Furthermore, we demonstrated that HspX is an effective adjuvant for antitumor vaccination using an in vivo cervical cancer model. The adjuvant increased the production of activated memory CD8<sup>+</sup> T cells in the spleen when HspX was used during E7 Ag recognition in DCs. The activated memory T cells induced and maintained the CTL activity specifically against the cancer expressing the E7 Ag. DC vaccination with the adjuvant HspX, compared with vaccination with only DCs, reduced the size of the cervical cancer and increased the survival rate.

Immunotherapy with vaccination can be more effective in the treatment of metastatic cancer, which is impossible to surgically remove. Metastatic cancers in the lung induced by the injection of B16-BL6 melanoma in mice were repressed by immunization with DCs that overexpressed the melanoma-associated Ag human gp100 (22). Similarly, we found that the injection of recognized DCs with tumor Ags reduced the extent of metastatic melanoma in the lungs. Furthermore, HspX potentiated the inhibitory effect of DCs when it stimulated the DCs as an adjuvant during Ag recognition. We also found that immunization with DCs stimulated with the Ag and/or HspX reduced regulatory T cell levels in the tumor and spleen (see Supplemental Fig. 3), which resulted in augmented cancer immunosurveillance. The mechanisms involved in the effect of DC immunization on the population of regulatory T cells require further investigation.

Immunotherapeutic designs based on DCs in cancer treatment are shifting to the development of more defined and safer vaccines. This has concomitantly created a growing demand for the use of immunopotentiators in DC-based immunotherapy, which are intrinsically poorly immunotargeted tumor Ags. In addition to facilitating the increased uptake of Ag by DCs, new immunoadjuvants are designed to facilitate the recruitment and activation of DCs by stimulating pattern recognition receptors, thereby enabling the transition from the innate to specific-adaptive immune system for tumor Ag-targeted T cell responses. Compared with earlier adjuvants, HspX has many advantages regarding safety, the optimal Th1 type T cell immunity, and dosage for ex vivo DC activation. HspX is clinically safe and defined, as it has been included in the BCG vaccines for several decades. Therefore, it has an advantage over other TLR4 agonists in drug development.

For example, monophosphoryl lipid A (MPLA) is a detoxified derivative of LPS from *Salmonella minnesota*, and is the first of a new generation of defined vaccine adjuvants to achieve widespread use in human populations since the approval of alum (23). Although LPS is highly toxic and causes strong inflammatory responses (24), the LPS derivative MPLA enhances adaptive immunity without causing excessive inflammation. The mechanism by which MPLA enables potent but safe adjuvanticity appears to be a result of biased TRIF signaling and selective activation of p38 MAPK (25). However, TRIF-biased TLR4 activation by MPLA may not produce the greatest Th1 immune response. Indeed, MyD88 and TRIF synergistic interactions are required for Th1 cell polarization by a TLR4-based adjuvant. As engagement of both the MyD88 and TRIF signaling pathways is essential for the effective adjuvant activity of HspX-mediated TLR4 activation, HspX is able to boost Ag-specific immunity elicited by DC-directed tumor Ags by signaling MyD88 and TRIF. In addition, our previous studies demonstrated that 5–10 µg/ml of recombinant mycobacterial Ags with

properties of TLR 2 or 4 agonists were required for optimal DC activation. By contrast, 500 ng/ml of HspX is sufficient for the functional activation of DCs.

In conclusion, we have shown that HspX is a potent and selective agonist of TLR4 and is highly effective in the induction of tumor-targeted Th1-type T cell immunity in DC-based cancer immunotherapy, using in vitro and in vivo models. The considerable effect of HspX as an immunoadjuvant will open avenues for the development of new immunotherapeutic strategies for better clinical outcomes.

## Disclosures

The authors have no financial conflicts of interest.

## References

- Grange, J. M., O. Bottasso, C. A. Stanford, and J. L. Stanford. 2008. The use of mycobacterial adjuvant-based agents for immunotherapy of cancer. *Vaccine* 26: 4984–4990.
- Banchereau, J., and A. K. Palucka. 2005. Dendritic cells as therapeutic vaccines against cancer. *Nat. Rev. Immunol.* 5: 296–306.
- Bansal, K., S. R. Elluru, Y. Narayana, R. Chaturvedi, S. A. Patil, S. V. Kaveri, J. Bayry, and K. N. Balaji. 2010. PE\_PGRS antigens of *Mycobacterium tuberculosis* induce maturation and activation of human dendritic cells. *J. Immunol.* 184: 3495–3504.
- Pecora, N. D., A. J. Gehring, D. H. Canaday, W. H. Boom, and C. V. Harding. 2006. *Mycobacterium tuberculosis* LprA is a lipoprotein agonist of TLR2 that regulates innate immunity and APC function. *J. Immunol.* 177: 422–429.
- Heo, D. R., S. J. Shin, W. S. Kim, K. T. Noh, J. W. Park, K. H. Son, W. S. Park, M. G. Lee, D. Kim, Y. K. Shin, et al. 2011. *Mycobacterium tuberculosis* Rv0462, induces dendritic cell maturation and Th1 polarization. *Biochem. Biophys. Res. Commun.* 411: 642–647.
- Jung, I. D., S. K. Jeong, C. M. Lee, K. T. Noh, D. R. Heo, Y. K. Shin, C. H. Yun, W. J. Koh, S. Akira, J. Whang, et al. 2011. Enhanced efficacy of therapeutic cancer vaccines produced by co-treatment with *Mycobacterium tuberculosis* heparin-binding hemagglutinin, a novel TLR4 agonist. *Cancer Res.* 71: 2858–2870.
- Byun, E. H., W. S. Kim, J. S. Kim, I. D. Jung, Y. M. Park, H. J. Kim, S. N. Cho, and S. J. Shin. 2012. *Mycobacterium tuberculosis* Rv0577, a novel TLR2 agonist, induces maturation of dendritic cells and drives Th1 immune response. *FASEB J.* 26: 2695–2711.
- Stewart, G. R., S. M. Newton, K. A. Wilkinson, I. R. Humphreys, H. N. Murphy, B. D. Robertson, R. J. Wilkinson, and D. B. Young. 2005. The stress-responsive chaperone alpha-crystallin 2 is required for pathogenesis of *Mycobacterium tuberculosis*. *Mol. Microbiol.* 55: 1127–1137.
- Roupie, V., M. Romano, L. Zhang, H. Korf, M. Y. Lin, K. L. Franken, T. H. Ottenhoff, M. R. Klein, and K. Huygen. 2007. Immunogenicity of eight dormancy regulon-encoded proteins of *Mycobacterium tuberculosis* in DNA-vaccinated and tuberculosis-infected mice. *Infect. Immun.* 75: 941–949.
- Geluk, A., M. Y. Lin, K. E. van Meijgaarden, E. M. Leyten, K. L. Franken, T. H. Ottenhoff, and M. R. Klein. 2007. T-cell recognition of the HspX protein of *Mycobacterium tuberculosis* correlates with latent *M. tuberculosis* infection but not with *M. bovis* BCG vaccination. *Infect. Immun.* 75: 2914–2921.
- Lin, K. Y., F. G. Guarnieri, K. F. Staveley-O'Carroll, H. I. Levitsky, J. T. August, D. M. Pardoll, and T. C. Wu. 1996. Treatment of established tumors with a novel vaccine that enhances major histocompatibility class II presentation of tumor antigen. *Cancer Res.* 56: 21–26.
- Inaba, K., M. Inaba, N. Romani, H. Aya, M. Deguchi, S. Ikehara, S. Muramatsu, and R. M. Steinman. 1992. Generation of large numbers of dendritic cells from mouse bone marrow cultures supplemented with granulocyte/macrophage colony-stimulating factor. *J. Exp. Med.* 176: 1693–1702.
- Wuyts, A., P. Menten, N. Van Osselaer, and J. Van Damme. 2004. Assays for chemotaxis. *Methods Mol. Biol.* 249: 153–166.
- Liu, Y. J. 2001. Dendritic cell subsets and lineages, and their functions in innate and adaptive immunity. *Cell* 106: 259–262.
- Willmann, K., D. F. Legler, M. Loetscher, R. S. Roos, M. B. Delgado, I. Clark-Lewis, M. Baggiolini, and B. Moser. 1998. The chemokine SLC is expressed in T cell areas of lymph nodes and mucosal lymphoid tissues and attracts activated T cells via CCR7. *Eur. J. Immunol.* 28: 2025–2034.
- Schilling, J. D., H. M. Machkovech, L. He, A. Diwan, and J. E. Schaffer. 2013. TLR4 activation under lipotoxic conditions leads to synergistic macrophage cell death through a TRIF-dependent pathway. *J. Immunol.* 190: 1285–1296.
- Ojaniemi, M., V. Glumoff, K. Harju, M. Liljeroos, K. Vuori, and M. Hallman. 2003. Phosphatidylinositol 3-kinase is involved in Toll-like receptor 4-mediated cytokine expression in mouse macrophages. *Eur. J. Immunol.* 33: 597–605.
- Koyasu, S. 2003. The role of PI3K in immune cells. *Nat. Immunol.* 4: 313–319.
- Hogquist, K. A., S. C. Jameson, W. R. Heath, J. L. Howard, M. J. Bevan, and F. R. Carbone. 1994. T cell receptor antagonist peptides induce positive selection. *Cell* 76: 17–27.
- Shi, C., L. Chen, Z. Chen, Y. Zhang, Z. Zhou, J. Lu, R. Fu, C. Wang, Z. Fang, and X. Fan. 2010. Enhanced protection against tuberculosis by vaccination

- with recombinant BCG over-expressing HspX protein. *Vaccine* 28: 5237–5244.
21. Peng, S., C. Trimble, L. Wu, D. Pardoll, R. Roden, C. F. Hung, and T. C. Wu. 2007. HLA-DQB1\*02-restricted HPV-16 E7 peptide-specific CD4<sup>+</sup> T-cell immune responses correlate with regression of HPV-16-associated high-grade squamous intraepithelial lesions. *Clin. Cancer Res.* 13: 2479–2487.
  22. Okada, N., Y. Masunaga, Y. Okada, H. Mizuguchi, S. Iiyama, N. Mori, A. Sasaki, S. Nakagawa, T. Mayumi, T. Hayakawa, et al. 2003. Dendritic cells transduced with gp100 gene by RGD fiber-mutant adenovirus vectors are highly efficacious in generating anti-B16BL6 melanoma immunity in mice. *Gene Ther.* 10: 1891–1902.
  23. Cluff, C. W. 2009. Monophosphoryl lipid A (MPL) as an adjuvant for anti-cancer vaccines: clinical results. *Adv. Exp. Med. Biol.* 667: 111–123.
  24. Przetak, M., J. Chow, H. Cheng, J. Rose, L. D. Hawkins, and S. T. Ishizaka. 2003. Novel synthetic LPS receptor agonists boost systemic and mucosal antibody responses in mice. *Vaccine* 21: 961–970.
  25. Mata-Haro, V., C. Cekic, M. Martin, P. M. Chilton, C. R. Casella, and T. C. Mitchell. 2007. The vaccine adjuvant monophosphoryl lipid A as a TRIF-biased agonist of TLR4. *Science* 316: 1628–1632.